PARAMETERS CONTROLLING NITRIC OXIDE EMISSIONS FROM GAS TURBINE COMBUSTORS

by

John B. Heywood and Thomas Mikus

Department of Mechanical Engineering
Massachusetts Institute of Technology
Cambridge, Massachusetts 02139

Presented at the

AGARD Propulsion and Energetics Panel

41st Meeting on

"Atmospheric Pollution by Aircraft Engines"

London, England

9-13 April 1973

PARAMETERS CONTROLLING NITRIC OXIDE EMISSIONS FROM GAS TURBINE COMBUSTORS

by

John B. Heywood and Thomas Mikus
Department of Mechanical Engineering
Massachusetts Institute of Technology
Cambridge, Massachusetts 02139 U.S.A.

SUMMARY

Nitric oxide forms in the primary zone of gas turbine combustors where the burnt gas composition is close to stoichiometric and gas temperatures are highest. It has been found that combustor air inlet conditions, mean primary zone fuel-air ratio, residence time, and the uniformity of the primary zone are the most important variables affecting nitric oxide emissions. Relatively simple models of the flow in a gas turbine combustor, coupled with a rate equation for nitric oxide formation via the Zeldovich mechanism are shown to correlate the variation in measured NO_x emissions. Data from a number of different combustor concepts are analyzed and shown to be in reasonable agreement with predictions. The NO_x formation model is used to assess the extent to which an advanced combustor concept, the NASA swirl can, has produced a lean well-mixed primary zone generally believed to be the best low NO_x emissions burner type.

1. INTRODUCTION

With the growth in air traffic, and the trend to bigger and higher pressure ratio gas turbine engines, aircraft emissions of oxides of nitrogen (NO_x) are expected to increase greatly over the next decade. Recent estimates suggest that by 1980, in the absence of emission controls, NO_x emissions will increase above their 1970 values by a factor of 2.2 at O'Hare Airport, 2.9 at John F. Kennedy Airport and 4.5 at Los Angeles International Airport[1]. As a consequence, the U.S. Environmental Protection Agency has proposed NO_x emission standards for aircraft turbine engines for January 1, 1979[2]. In addition, the effect of NO_x emissions from a fleet of SST's in the stratosphere on the ozone layer is a topic of intensive study and debate[3]. There is an urgent need to understand the factors governing NO_x emissions from aircraft gas turbine engines, and use that understanding to develop combustor designs with much reduced emissions.

It is well known that jet aircraft NO_x emissions are most important at high engine power settings. Thus take-off and landing are the primary operating modes of concern for subsonic aircraft. For the SST, NO_x emissions during cruise in the stratosphere are of greatest concern. Experimentally it has been found that increases in combustor air inlet temperature and pressure, and thus engine compressor pressure ratio, increase NO_x emissions. For a given engine operating condition, it is known that the fuel injection technique, the geometry of the combustor liner, and the pressure drop across the liner all affect NO_x emissions[4][5].

The oxides of nitrogen which leave the engine are nearly all nitric oxide, NO, with only a few percent nitrogen dioxide, NO_2. Several models for predicting the formation of NO inside actual gas turbine combustors have already been developed[6]-[10]. These models have established that the exhaust NO concentration depends on rate-limited reactions occurring in the burning gases in the high temperature zones of the combustor. As additional air is mixed with the combustion products to cool the gases before entry to the turbine, the NO formation chemistry freezes. After this point, the NO concentration only changes due to dilution. In this paper, we will review how NO is formed in aircraft gas turbine combustors, and relate the combustor design parameters listed above to the thermodynamic variables which control the NO formation process.

We will then show that relatively simple models which include only the major parameters affecting NO formation can be used to predict NO_x emissions. The agreement obtained to date with predictions from such models and experimental data from conventional combustors will be reviewed. This type of model is then applied to the NASA swirl can combustor[11] and it is shown why this concept offers a significant reduction in NO_x emissions. To illustrate the usefulness of such models, predictions are then made for a swirl can combustor at take-off conditions for a JT9D or CF-6 engine.

Our intent in this review is to demonstrate that simple models of the type we describe can predict NO_x emissions with sufficient accuracy to be useful in the design process. The model can be used to extrapolate test data from a combustor on a test stand to actual engine operating conditions. By identifying the key design parameters which affect NO formation, and quantifying the effect on emissions of changing these parameters, such models can provide a structure for a combustor development program. With these goals our emphasis will be on relatively simple models which can easily be adapted to different types of combustors.

The results presented here come from our own group at M.I.T.[7][12][13] and from work at Northern Research and Engineering Corporation[6][8]. As a result of close collaboration, the models developed by these groups are conceptually similar and differ only in detail. The two groups have also analyzed different types of combustors, and an extensive model evaluation can therefore be carried out.

2. MODEL DESCRIPTION

2.1 Combustor Flow Characteristics

Most of the models proposed for predicting NO_x emissions from combustors contain two parts. The first is a kinetic scheme for nitric oxide formation, developed from a plausible physical description of

the turbulent flame structure within the primary combustion region. The second part is a fluid mechanic model which couples the NO kinetics to those aspects of the flow field which affect the NO formation process. Before each of these parts of the model is discussed in detail, the general nature of the flow in a conventional combustor will be reviewed.

The main features of the flow in a conventional annular jet engine combustor are shown in Figure 1. Both can and annular combustors can be divided roughly into two parts, a primary and a secondary zone. In the primary zone, at high power conditions, about 90 percent of the fuel is burnt and the mean fuel-air ratio is slightly rich of stoichiometric (equivalence ratio between about 1 and 1.5). To reduce gas temperatures to an acceptable level at turbine inlet, the overall equivalence ratio must be reduced to about 0.25. Thus only 20 to 25 percent of the total combustor airflow enters the primary zone.

Figure 1 indicates schematically the mean flow pattern in the combustor. Though a mean flow pattern in any given combustor is discernible from water analog studies, substantial fluctuations and unsteadyness occur. In the primary zone, the swirler air and the air jets through the first row of holes set up the recirculating flow pattern which stabilizes the flame. These air jets also vigorously mix the primary zone gases to obtain adequate distribution of the fuel.

In the secondary zone, the remaining air is mixed with the primary zone combustion products to complete combustion of the fuel, and cool the gas stream to the temperature distribution required at turbine inlet. About two-thirds of the secondary zone air enters the combustor transverse to the internal flow through large holes in the liner and mixes in the bulk of the flow. About one-third of the secondary zone air enters parallel to the liner through slots to film cool the combustor walls. The flow is primarily unidirectional.

2.2 Kinetics of Nitric Oxide Formation

At the temperatures and equivalence ratios found in all types of burners, NO forms via the extended Zeldovich mechanism:

$$O + N_2 \rightleftharpoons NO + N \tag{1}$$

$$N + O_2 \rightleftharpoons NO + O \tag{2}$$

$$N + OH \rightleftharpoons NO + H \tag{3}$$

Reaction (1) is endothermic left to right and relatively slow. Reactions (2) and (3) are exothermic and fast. In the absence of dilution the rate of change of NO concentration in a fluid element of volume V is

$$\frac{1}{V}\frac{d[NO]V}{dt} = k_1[O][N_2] - k_{-1}[NO][N] + k_2[N][O_2] - k_{-2}[NO][O] + k_3[N][OH] - k_{-3}[NO](H] \tag{4}$$

where [ ] denote concentrations in gram moles/cm^3, and $k_{\pm i}$ are the forward and reverse rate constants of the ith reaction.

Before equation (4) can be used to calculate NO formation rates, two questions must be resolved: (i) the method for calculating [N], and (ii) the method for calculating [O], [O_2], [OH] and [H]. The N_2 concentration is essentially constant. The appropriate assumptions depend on the pressure, temperature and atomic composition of the system being analyzed. We are concerned here with typical gas turbine combustor conditions, i.e. pressures ~ 15 atm, peak temperatures ~ 2500 °K, residence times at these peak conditions ~ 3 msec, equivalence ratio for hydrocarbon - air combustion between about 0.7 and 1.3.

Since the N atom mole fraction is of order 10^{-8}, the steady state approximation is usually made for [N]. This is a standard procedure in treating reacting mixtures whenever a species is present in very small amounts compared with species of interest.

The second question of the radical and O_2 concentrations is more complex, and a model for the flame front in the combustor must be formalized before appropriate assumptions can be made. Heywood[13] and Westenberg[14] have justified the assumption that under appropriate conditions, the O, O_2, OH and H concentrations are the equilibrium values. The argument can be summarized as follows.

In a premixed one-dimensional flame, there is a thin initial reaction zone where radicals are generated and react with the hydrocarbon fuel. Most of the temperature rise occurs in this zone. This region is followed by a thicker zone where CO is oxidized to CO_2, and radicals present in greater than equilibrium concentrations recombine through termolecular reactions. If the NO formed in this nonequilibrium region is much less than the amount formed downstream of the flame, then the O, OH, H and O_2 equilibrium assumption is a reasonable approximation. We have recently completed studies of CO equilibration in the flame zone at pressures, temperatures and equivalence ratios typical of a combustor primary zone[15]. These studies show that equilibration times are less than 10^{-4} sec. (for equivalence ratios between 0.7 and 1.3) which is much less than typical primary zone residence times, and that the effect of radical concentrations above equilibrium values will not be significant on NO formation. The amount of NO formed in the reaction zone of the flame is small compared with the amount formed downstream of the flame at gas turbine combustor conditions.

With these assumptions for [N], and [O], [OH], [O_2] and [H] equation (4) can be rearranged to give[12]

$$\frac{d\{NO\}}{dt} = \frac{2M_{NO}}{\rho}\frac{(1-\alpha^2)R_1}{(1+\alpha K)} \tag{5}$$

where {NO} is the nitric oxide mass fraction, M_{NO} is the molecular weight of NO, ρ is the gas density, α is $\{NO\}/\{NO\}_e$ and subscript e denotes the equilibrium value, R_i is the one-way equilibrium reaction rate for reaction (i) (e.g. $R_1 = k_1[O]_e[N_2]_e = k_{-1}[N]_e[NO]_e$) and $K = R_1/(R_2 + R_3)$. Expressions for the rate constants for reactions (1) - (3), and typical values for R_1, R_2, R_3 and K are given in Table 1.

TABLE 1

Values of One-way Equilibrium Reaction Rates for Extended Zeldovich Mechanism

($T = 2500$ °K, $p = 10$ atm, $\phi = 1.0$)

	rate const., k_i*	ref.	R_i**
R_1	$1.4 \times 10^{14} \exp(-75{,}400/RT)$	(16)	2.1×10^{-5}
R_2	$6.4 \times 10^{9}\ T \exp(-6250/RT)$	(16)	5.5×10^{-6}
R_3	4.2×10^{13}	(17)	2.9×10^{-5}
$K = R_1/(R_2 + R_3)$			0.61

*units: $cm^3\ mole^{-1}\ sec^{-1}$

**units: $mole\ cm^{-3}\ sec^{-1}$, except K.

Since K is of order 1, for $[NO] \ll [NO]_e$ (i.e. $\alpha \ll 1$) the rates of reactions (2) and (3) have little effect on the NO formation rate. Either reaction provides a fast path to convert the N atom produced in reaction (1) to NO. As [NO] approaches $[NO]_e$ the value of K starts to affect the NO formation rate. For lean mixtures $R_2 \sim R_3$, and the inclusion of reaction (3) makes little difference. For rich mixtures $R_3 \gg R_2$. Heywood[13] has shown that the omission of reaction (3) from the scheme results in an underestimate of the NO formation rate by a factor of 2 for a stoichiometric mixture with $\alpha \approx 0.5$.

Equation (5) shows that the NO formation rate depends only on the pressure, temperature, atomic composition and NO concentration downstream of the thin flame zone. NO profiles calculated with equation (5) as a function of time downstream of a one-dimensional flame for a stoichiometric mixture are shown in Figure 2. Since primary zone residence times are of order 3 msec and peak temperatures ~ 2500 °K, we would not expect NO concentrations to reach equilibrium levels within the high temperature zone of a gas turbine combustor.

Changes in equivalence ratio at a given temperature do not change the time required to equilibrate NO[12], but do substantially change the formation rate as shown in Figure 3. The gas turbine combustor is essentially adiabatic; the local flame temperature therefore depends only on the inlet air conditions and the local equivalence ratio. The dashed line in Figure 3 indicates the path a burnt gas eddy or pocket would follow as it is diluted in its passage through the combustor. NO formation rates peak sharply at $\phi = 1.0$, and rapid freezing of the NO forming reactions occurs as the mixture is then leaned out. Obviously those regions of the combustor where the burnt gas composition is close to stoichiometric are the regions where most of the NO is formed.

2.3 Fluid Mechanic Models

To develop a fluid mechanic model for the primary zone, we must now relate this description of a premixed one-dimensional flame to the flame structure in a conventional gas turbine combustor. Fuel as a liquid spray and air enter the primary zone separately in approximately stoichiometric proportions. The fuel droplets vaporize as they move relative to the primary zone gases in a time of order 2 msec[18] leaving fuel vapor rich wakes which then mix with air and already burnt gas and burn. Mixing of fuel and air to a uniform equivalence ratio would not be expected. As the fuel droplets vaporize, fuel vapor and air mix and form turbulent eddies or pockets of combustible mixture with a wide range of fuel-air ratios.

High speed movies of liquid fueled combustors and burners suggest that the thin flame front model described above is still applicable. In such combustors both nonluminous flame fronts propagating through eddies of fuel vapor and air which are essentially premixed, and soot forming luminous flames surrounding rich fuel vapor air eddies can be observed[19]. Such an unsteady turbulent flame structure would be expected in the vigorously stirred primary zone where fuel and air enter separately. As each eddy containing fuel vapor and air ignites, either a thin flame front will propagate through the eddy, or envelope and consume the eddy, depending on the local fuel-air ratio and eddy size. Both "premixed" and "diffusion controlled" burning would be expected. As a consequence, burnt gas eddies are produced with a distribution in fuel-air ratio about the mean primary zone value. This distribution will change with time as these eddies mix with each other, and with dilution air, through the action of turbulence and molecular diffusion. One expects the details of the fuel injection process (which determine droplet sizes and the distribution of droplets within the primary zone) and the air flow pattern (which determines the mixing intensity) to affect both the initial spread of the eddy fuel-air ratio distribution and its change with time. This physical description of the combustion process is the basis for the model we will now describe.

Several flow models for gas turbine combustors have been presented in the open literature[6][9][10][20] and [21]. These have recently been reviewed by Mellor[18]. We will concentrate on the simplest model which has been compared extensively with experimental data. In this model, developed by Fletcher

and Heywood[6] and the authors[7], no attempt is made to describe the details of the turbulent flow field. The primary zone of the combustor is treated as a partially stirred reactor. It is assumed that the fuel and air which enter the primary zone are rapidly dispersed throughout the zone to form discrete fluid elements or eddies of a scale small compared with combustor dimensions. We will assume these eddies are uniformly dispersed throughout the zone volume, and after combustion the gas within each eddy remains essentially together throughout its residence time in the primary zone. For such a partially stirred reactor model it can be shown that the fraction of the flow with residence time between t and t + dt is given by $\psi(t)dt$ where

$$\psi(t) = (1/\tau)\exp(-t/\tau) \tag{6}$$

and τ, the mean residence time, is the primary zone volume divided by the volume flow rate of burnt gas out of the zone.

But since the fuel and air are not uniformly mixed, different burnt gas elements will have different average equivalence ratios during their residence time in the primary zone. A Gaussian distribution about the mean equivalence ratio $\bar{\phi}$ (or mean fuel mass fraction which is almost equivalent[6]) is assumed; i.e., the fraction of the flow with equivalence ratio (or fuel fraction) between ϕ and $\phi + d\phi$ is given by $f(\phi)d\phi$ where

$$f(\phi) = (1/\sigma\sqrt{2\pi})\exp[-(\phi - \bar{\phi})^2/2\sigma^2] \tag{7}$$

and σ is the standard deviation. A mixing parameter s, where

$$s = \sigma/\bar{\phi} \tag{8}$$

is used as a measure of the nonuniformity of the primary zone; s = 0 corresponds to perfect mixing. The mean primary zone equivalence ratio, $\bar{\phi}_p$, is determined from the fuel and air flows into the primary zone. Approximate correlations are available for estimating the fraction β of the fuel entering the primary zone which burns there[22]. Techniques have been developed for estimating the air flow distribution within the combustor liner[23].

The importance of characterizing the uniformity of mixing is shown in Figure 4. Mean NO formation rates (for $\{NO\} << \{NO\}_e$) are shown as a function of mean primary zone equivalence ratio for combustor air inlet conditions of 843°K and 24.1 atm for s = 0, 0.25 and 0.5. For stoichiometric mixtures, the mean NO formation rate is substantially reduced as the primary zone becomes less uniform; for rich ($\bar{\phi} \geq 1.1$) and lean ($\bar{\phi} \leq 0.8$) the mean NO formation rate is substantially increased. Note that the peak NO formation rate shifts to the lean side as s increases.

The remainder of the combustor, the secondary zone, is usually treated as a one dimensional flow with air addition. The importance of this zone in predicting exhaust NO_x emissions depends on the mean primary zone fuel-air ratio. Where most of the primary zone flow is stoichiometric or lean, addition of dilution air cools the burnt gases close to the primary zone exit and rapidly quenches the NO forming reactions as indicated in Figure 3. Mikus and Heywood[7] in their treatment of this type of burner made the reasonable assumption that the effect of the dilution air at the start of the secondary zone is to quench immediately the NO forming reactions. The NO mass fraction at burner exit is just the mean NO mass fraction at primary zone exit times the ratio of primary zone mass flow rate to total mass flow rate.

If a substantial part of the primary zone flow is fuel rich, this simplifying assumption is no longer valid. As rich burnt gas eddies mix with dilution air or leaner eddies and pass through the stoichiometric fuel air ratio, NO formation rates peak as shown in Figure 3. The rate of dilution is therefore an important parameter.

The approach taken by Fletcher, et al.[6][8] was to specify the change in mean fuel mass fraction F (F = mass fuel/total mass) and mixing parameter s along the length of the secondary zone as eddies of diluting air and burnt gases mix and react, and any fuel not burnt in the primary zone is consumed. A simple eddy mixing model was used to take account of changes in NO concentration due to mixing. Since in typical aircraft turbine combustors, the NO concentrations in the stoichiometric regions of the combustor are about one third or less of the equilibrium level, changes in local NO concentration due to mixing have little effect on the NO formation rate (see equation (5)). The mean equivalence ratio profile along the length of the secondary zone is determined from the air flow through the liner. The flow through film cooling slots and dilution air holes in the liner can be calculated using standard techniques[23] and a plot of total mass flow in the liner as a function of length obtained. The average equivalence ratio across the cross section of the can is estimated by smoothing this plot. The variation of s along the combustor is discussed more fully in the next section. Only the first part of the secondary zone ($\bar{\phi} \geq 0.6$ for a conventional combustor) is important. In the downstream section only dilution of previously formed NO occurs.

These models have been programmed for solution on a digital computer. Equation (5) is linked with a program for calculating equilibrium thermodynamic properties and species concentrations of kerosene-air burnt gas mixtures for given pressure, temperature and atomic composition. Equation (5) can be integrated to give {NO} as a function of time for any burnt gas element. Suitable averaging over the residence time distribution, equation (6), and equivalence ratio (or fuel mass fraction) distribution, equation (7), yield the average nitric oxide concentration at primary zone exit. The two distributions are assumed statistically independent. In the dilution zone, the calculation procedure follows burnt gas eddies of given equivalence ratio along the burner in incremental steps. The mean NO mass fraction is found by weighting the NO mass fraction in eddies of different equivalence ratio according to equation (7). In each subsequent step along the burner, allowance is made for the change in NO mass fraction in each eddy due to mixing. The additional NO formed is then computed for a number of eddies of different equivalence ratio, and a new average NO mass fraction calculated. Because the eddy temperature and radical concentrations used are the equilibrium values, they depend only on equivalence ratio and initial air conditions. And since {NO} is usually significantly less than $\{NO\}_e$, the effects of mixing (which changes s and $\bar{\phi}$) can be accounted for with this approximate calculation procedure.

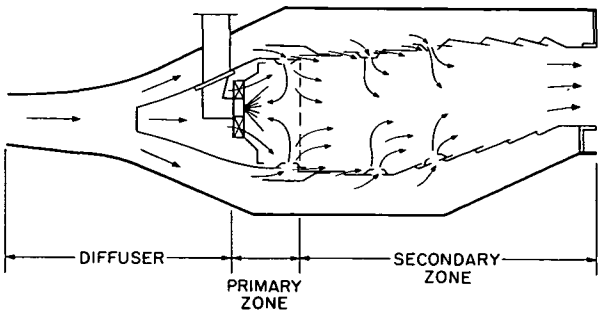

Fig. 1. Cross-section of typical annular gas turbine combustor showing mean flow pattern.

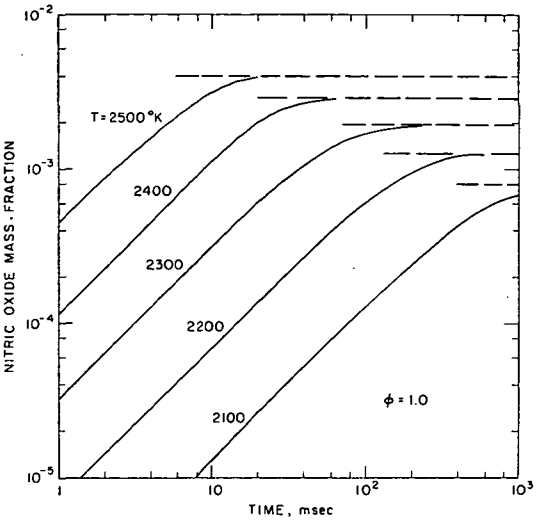

Fig. 2. Calculated NO mass fractions as function of time after combustion for different temperatures for a one-dimensional premixed flame. C_NH_{2N}-air mixture, pressure 10 atm, equivalence ratio 1.0. Dashed lines are equilibrium NO mass fractions.

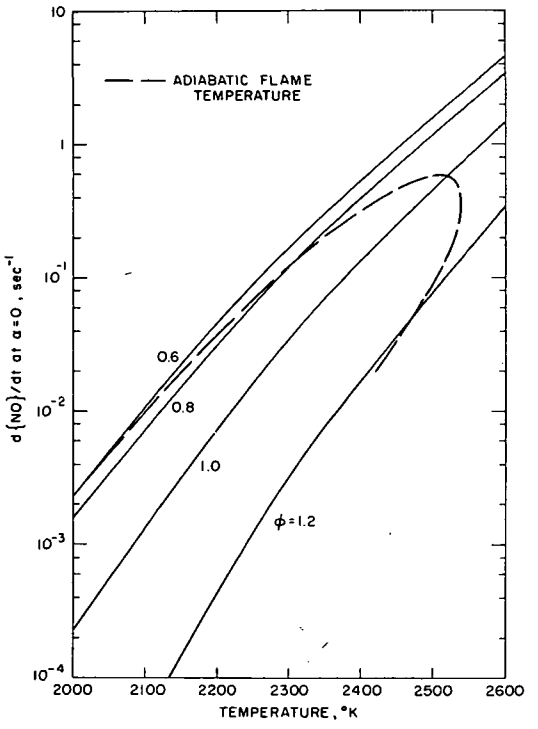

Fig. 3. NO formation rate, mass fraction per sec., for $\alpha = 0$ as a function of temperature for different equivalence ratios and 15 atm pressure. Dashed curve shows adiabatic flame temperature for kerosene combustion with 700 °K, 15 atm, air.

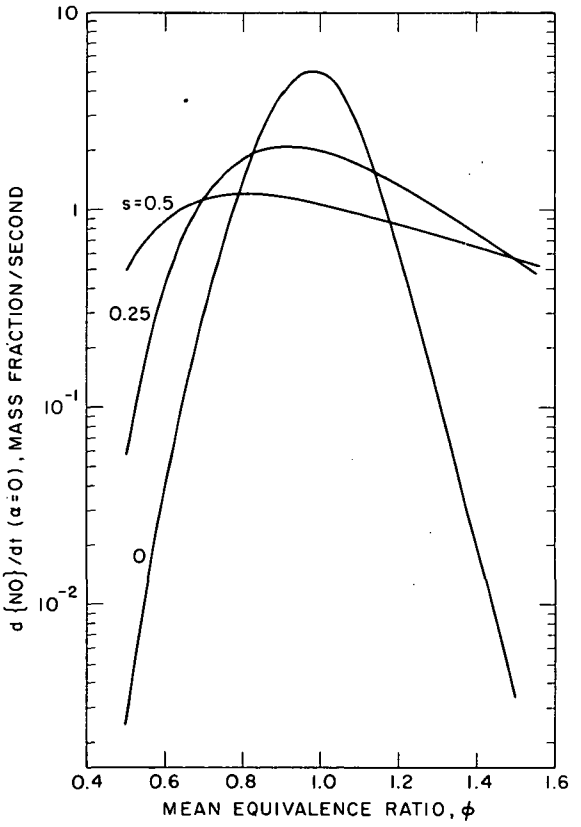

Fig. 4. Average NO formation rate for nonuniform kerosene-air burnt gas mixtures with different mean equivalence ratios and mixing parameters, s. Air conditions: 843 °K, 24 atm.

3. MODEL EVALUATION

3.1 Sources of Uncertainty in Model Calculations

The previous sections indicate that the important model parameters are: air inlet temperature and pressure, T_a and p_a; the mean equivalence ratio of the burnt gases in the primary zone, $\bar{\phi}_p$; the mixing parameter in the primary zone, s_o; and the rate of air addition in the early part of the secondary zone. With the exception of s, values of these parameters can be estimated for conventional combustors. However, before we examine the relationship of these parameters to predictions of combustor NO_x emissions, the major uncertainties in the model will be discussed.

The expresisons used for rate constants are one possible source of error. Baulch, et al.[16] give an uncertainty for k_1 as listed in Table 1 of ± a factor of two up to 1600 °K increasing to a factor of four at 5000 °K. Examination of equation (5) shows that uncertainties in k_2 and k_3 are much less important. The uncertainty in {NO} is thus approximately proportional to the uncertainty in k_1, when, as is usually the case, the NO concentration in the highest temperature zones in the combustor do not approach equilibrium levels. The omission of radiation heat transfer is also a possible source of error in calculating the NO formation rate. While a gas turbine combustor is regeneratively cooled because the liner cooling air is eventually mixed with bulk flow, radiative heat losses from the gas in the primary and early part of the secondary zone will reduce peak burnt gas temperatures. In the primary zone, most of the radiation comes from soot particles formed in fuel-rich regions of the flame. Thus one expects error introduced by the omission of radiation from the primary and secondary zone models to be most significant in combustors with fuel-rich poorly mixed primary zones. The radiation heat flux to the liner wall will depend on the flame temperature and the amount of soot formed within the flame zone.

$\bar{\phi}_p$ depends on measured fuel flow rate, estimated air flow into the primary zone and an estimate of the fraction of the fuel fed to the primary zone which burns there. The latter estimate is the most suspect, and existing correlations are probably inadequate. The correlation[22] used by Fletcher, et al.[8] relates the primary zone combustion efficiency β to the primary zone fuel load factor, $\dot{m}_f/V_p p^2$, where $\dot{m}_f$ is the fuel flow rate, V_p is the primary zone volume and p the pressure level. The flame structure discussion in Section 2.3 suggests that the mixing characteristics would also be important. For the same fuel load factor, a better mixed primary zone will have a higher combustion efficiency.

The mixing parameter s must, as yet, be determined empirically by matching experimental NO_x emissions data. The dependence of s on fuel injection and air flow characteristics is examined in Section 3.4. More quantitative relationships for evaluating s are now being developed.

The quenching rate of the primary zone gases with dilution air, and the rate of burn up of fuel which leaves the primary zone unburnt must also be estimated. Fletcher, et al.[8] carried out a sensitivity analysis to examine the effect of variations in these factors about their assumed average values and concluded that possible errors are quite small (≤ 25 percent). The fact that mixing with dilution air does not occur uniformly is not important in predicting overall NO emissions. The additional NO formed in burnt gas elements which are quenched more slowly than the mean compensates for elements quenched more rapidly than the mean since the combustor is almost adiabatic and the local NO formation rate is only weakly dependent on local NO concentration.

A comparison of model calculations with measured NO_x emissions from several combustors will now be made. Provided the absolute magnitude of the data can be predicted within about a factor of ±2, accurate prediction of the trends in the data is the more important test of model usefulness. The uncertainties in some model input parameters, and some of the approximations made preclude any expectation of more precise agreement.

3.2 Effects of Air Fuel Ratio, Air Inlet Temperature and Pressure

An extensive evaluation of the type of model described in Section 2 has been carried out by Fletcher, et al.[8] Two combustors with different characteristics were tested over a range of operating conditions, and measured and predicted NO emissions compared. Tests were carried out with one operating variable changed at a time which does not correspond to normal combustor operation in a jet engine, but does facilitate model evaluation.

Figure 5 shows measured NO concentrations at combustor exit and the results of model calculations for two combustors A and B[8]. Each combustor was operated with inlet air at 85 psia and 700 °K and essentially constant air flow rate over a range of fuel flow rates. The measured emission characteristics of the two combustors are quite different, combustor A showing a more rapid decrease in emissions as air fuel ratio (AFR) increases. The solid lines show model predictions with constant values of s_o and with the primary zone burnt fuel fraction β given by the correlation in ref. (22). For combustor B, the $s_o = 0.7$ line is a good match to the data over the AFR range 55 to 130. For combustor A, the $s_o = 0.3$ curve matches the slope of the data but falls below the measurements. However, as explained in Section 3.1 the correlation used for β does not take account of differences in primary zone mixing characteristics. Jackson and Odgers, in their discussion of factors influencing heat release, recognized the importance of pressure loss factor on combustor efficiency,[22] but since pressure loss factor is relatively constant for gas turbine combustors they developed a single correlation. For the same fuel loading factor in the primary zone, better mixing should increase the value of β. Thus a correlation for β appropriate for $s_o = 0.3$ should give higher values than a correlation for $s_o = 0.7$. The scatter in the data used to develop the β correlation underline its approximate nature. β was treated as an adjustable parameter,[8] and increasing β by 15 percent gives the dashed line in Figure 5 which matches the data over the AFR range 50 to 85. The idle NO emissions at an AFR of about 140 probably originate in the pilot flame.

The different NO emission chracteristics of these two combustors can be explained as follows[8]. Combustor B burns with a rich primary zone for AFR less than about 70. Combustor A burns with a lean primary zone throughout its operating range. Though combustor A has a small primary zone with a higher loading factor than B, the primary zone combustion efficiencies (between 0.75 and 0.85) are similar since

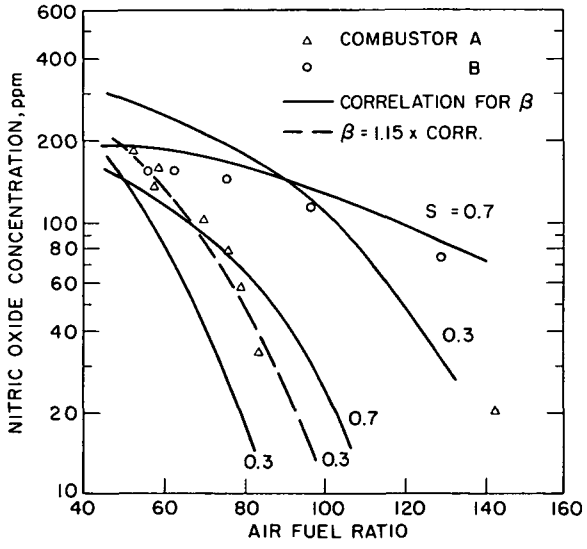

Fig. 5. Comparison of measured and predicted NO concentrations at combustor exit for two can combustors A and B for a range of overall air fuel ratios. Kerosene fuel, 700 °K, 85 psia air. s is primary zone mixing parameter. β is fraction of fuel fed to primary zone which burns there. From Fletcher et al.(8)

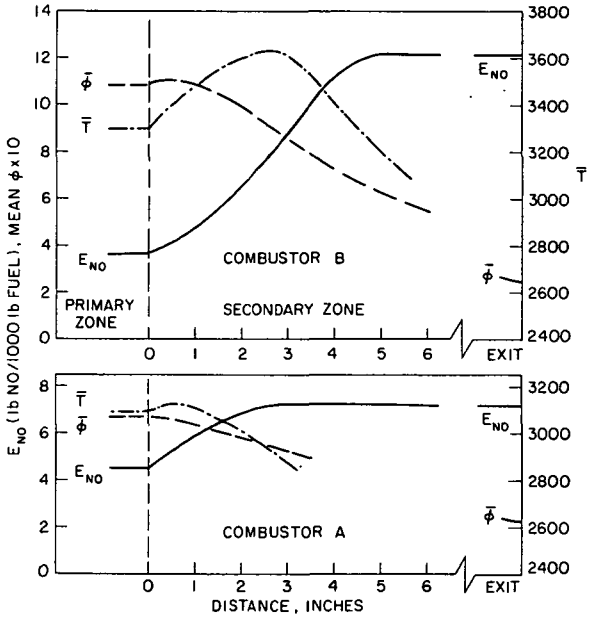

Fig. 6. Calculated average burnt gas temperatures $\bar{T}$ and equivalence ratios $\bar{\phi}$, and NO emission index along the length of two can combustors A and B. A has a fuel-lean and B a fuel-rich primary zone. From Fletcher et al.(8)

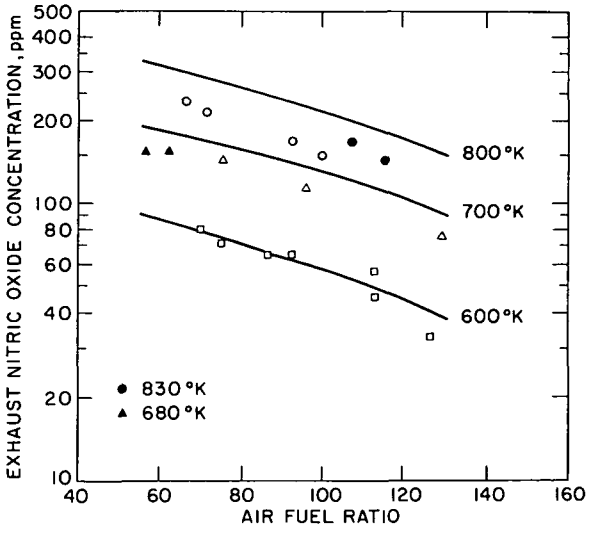

Fig. 7. Comparison of measured and predicted NO concentrations at burner exit for combustor B for a range of overall air fuel ratios and air inlet temperatures. Pressure is 85 psia. Predictions are for s_o = 0.7 and average air dilution rate. From Fletcher et al.(8)

A is better mixed.

This difference in emission characteristics is further illustrated in Figure 6 which shows calculated average burnt gas temperatures, $\bar{T}$, average burnt gas equivalence ratio $\bar{\phi}$, and NO emission index E_{NO} along the length of the two combustors[8]. The NO emission index is lb NO/1000 lb fuel. It represents the amount of NO formed upstream of any axial position and indicates that the NO chemistry is frozen at an equivalence ratio of about 0.6. However, the NO concentration continues to decrease along the length of the combustor due to dilution. The conditions for each calculation are given in the figure caption. As a consequence of the partially stirred reactor primary zone model, $\bar{T}$, $\bar{\phi}$ and E_{NO} are constant within the primary zone.

In combustor B at the operating condition shown only one third of the exhausted NO is formed in the primary zone. Thus the rate of dilution of the gases just downstream of the primary zone has an important effect on total emissions. In combustor A with a lean primary zone, about two thirds of the exhausted NO is calculated as originating in the primary zone. When β is increased as described above to obtain a better match with the measured data, a higher fraction of the total NO originates in the primary zone. Thus the rapid quench assumption for a combustor with a lean well mixed primary zone which has been used by the authors[7] is a reasonable simplification.

The results of gas sampling and analysis inside the secondary zone of combustor B[8] lend support to these calculated profiles. Although a radial NO concentration gradient was measured at two axial locations (x = 3 and 7 inches) in the secondary zone, cross section average measured values were in close agreement with calculated mean values. The measured NO concentrations increase by about a factor of 2.5 from the edge of the film cooling layer to the can axis. These nonuniformities in time averaged NO concentrations presumably result from nonuniform dilution rates within the secondary zone.

The observed difference in NO emission characteristics with decreasing load (increasing AFR) for combustors with fuel-rich or fuel-lean primary zones is consistent with the variation in average NO formation rate shown in Figure 4. As the primary zone is leaned out (approximately in proportion to overall AFR), the average NO formation rate for the s_o values used above decreases substantially only after the primary zone becomes quite lean.

The effect of variations in combustor inlet air temperature at constant pressure on NO emissions for combustor B is shown in Figure 7[8]. The solid lines are calculations based on an average secondary zone dilution rate obtained by smoothing a plot of air flow through the liner wall versus distance to allow for the delay in bulk mixing. The same value of s_o matches the measured data trends as overall AFR is increased. However, the effect of increasing air inlet temperature is overpredicted; a possible cause is omission of radiation heat losses in determining the burnt gas temperatures.

Data from Norster and Lefebvre[24] can be used to estimate the temperature drop below adiabatic flame temperatures resulting from radiation heat losses. Peak burnt gas temperatures would be about 20 °K below the adiabatic flame temperature with 600 °K inlet air, and 30 °K below with 800 °K inlet air for combustor B at an AFR of 65 and other conditions appropriate to Figure 7. An estimate of the change in NO formation rate resulting from these temperature decreases indicates the 800 °K air line would then lie about 24 percent lower and the 600 °K line about 10 percent lower at an AFR of 65. These approximate calculations support the conclusion that radiation heat losses account for the difference between measured and predicted effects of air inlet temperature.

The model also predicts the effect of changes in inlet air pressure. Experimental data show that, for a given combustor with fixed inlet air temperature, overall air fuel ratio and reference velocity, the NO emissions increase as the square root of air pressure[5]. Equation (5) can be rearranged to show this dependence. Since the reaction

$$O + O + M \rightleftharpoons O_2 + M \tag{9}$$

is in equilibrium,

$$[O] = \frac{x_o \rho}{M} = \left(\frac{x_{o_2}}{K_p p}\right)^{1/2} \tag{10}$$

where x_i is the mole fraction of species i, M is the molecular weight of the burnt gas mixture and K_p is the equilibrium constant for reaction (9). Using the perfect gas law, equation (5) can then be rearranged to give

$$\frac{d\{NO\}}{dt} = \frac{2M_{NO}\, k_1\, x_{N_2}}{M R T}\left(\frac{x_{o_2} p}{K_p}\right)^{1/2} \frac{(1 - \alpha^2)}{(1 + \alpha K)} \tag{11}$$

where R is the universal gas constant. For typical values of s_o for conventional combustors, Figure 3 shows the maximum NO formation rate occurs on the lean side of stoichiometric where x_{o_2} is essentially independent of pressure. For a fixed inlet air temperature, the burnt gas temperature T, k_1 and K_p only vary weakly with pressure. For $\alpha \lesssim 0.5$ which is usually the case, equation (11) shows that $d\{NO\}dt$ increases as $(p)^{1/2}$. Thus for the same reference velocity, NO emissions will also vary approximately as $(p)^{1/2}$.

3.3 Predicting Emissions from the GM GT-309 Engine

The model can be fitted into an engine cycle and used to calculate NO emissions over the load range of an engine. Here air flow rate, air fuel ratio and combustor air inlet conditions all vary

simultaneously. The authors[7] have applied this model to the General Motors GT-309 regenerative gas turbine[25][26] and compared predicted and measured NO emissions.

The GT-309 prototype engine has a can-type combustor with air-atomizing fuel injection. It has a well-defined primary zone because most of the dilution air is added at one axial station. Since the primary zone is operated at fuel-lean conditions, the assumption of rapid quenching of nitric oxide formation at the primary zone exit is a reasonable approximation, greatly simplifying the nitric oxide analysis.

The fraction of the total air flow through the combustor which enters the primary zone and takes part in primary zone combustion can be estimated from the sizes of the various orifices in the combustor liner and the approximate percentage of liner cooling air entrained into the primary flow. The mean primary zone equivalence ratio, obtained from the fuel flow and calculated primary air flow, is less than unity for all engine operating conditions. At each operating point a mean primary zone residence time, based on the volume flow rate at primary zone conditions, is calculated. Table 2 lists the values of combustor parameters over the engine's operating range.

TABLE 2

Data Used in GT-309 NO Emissions Study

Gasifier turbine speed %	Combustor inlet Temperature °F	Combustor inlet Pressure atm	Mean primary zone Equivalence ratio	Mean primary zone Residence time, msec
100	1091	3.68	0.81	6.8-7.3
90	1154	3.08	0.72	6.9-7.3
80	1233	2.53	0.62	7.2-7.5
70	1314	2.08	0.52	7.7-7.8
60	903	1.70	0.28	9.8
50	964	1.44	0.22	11.2

Treating the primary zone as a partially-stirred reactor, as described in Section 2.3, with 100% combustion efficiency and no heat losses, allows a computer analysis of nitric oxide formation with only one free parameter, the mixing parameter s. Figure 8 compares calculated NO concentrations at combustor exit with engine measurements. With $s \simeq 0.5$ the calculations match the measured trends reasonably well from part load to full load (70-100 percent gasifier speed). The poor match of the uniformly mixed primary zone calculations (the $s = 0$ line) with the measured data underlines the importance of including nonuniformities in the NO formation model.

At lower gasifier speeds (50-55 percent) corresponding to idle, the model described here predicts NO concentrations orders of magnitude below the measured values. At the low gasifier speeds corresponding to idle and low power output modes, fuel and air flow rates are far away from the design point. The flow pattern and level of turbulence within the primary zone become radically different; considering the entire primary zone as a stirred reactor is no longer valid. Equivalence ratio and residence time distributions based on air flow rate for the whole primary zone are no longer good approximations to actual combustion conditions.

Results of tests on two modifications of the standard GT-309 burner with earlier quenching of the primary zone combustion products have been reported by Cornelius and Wade[26]. The full power exhaust NO concentrations, relative to the standard burner are shown in Figure 9 as a function of relative residence time. The model predictions for $0 < s < 0.5$ are in close agreement; the value of s only weakly influences the relative effect of changes in residence time. This comparison does, however, support the conclusion that NO concentrations in the primary zone are below equilibrium levels.

3.4 The Mixing Parameter s

So far s has been treated as a floating parameter whose value is determined by matching predictions to measured emissions data. It has been found that a constant value of s_o in the primary zone can be used for a given combustor over a wide range of operating conditions and gives acceptable NO predictions. But different types of combustors require different values of s_o, and it is obvious that a better understanding of the relation of s to design and operating variables is required. Pompei and Heywood[27] have developed a more quantitative model for s in a kerosene fueled atmospheric pressure cylindrical burner which has several features in common with a gas turbine combustor. A high pressure air-assist atomizer was used to inject the fuel. For the same total air and fuel flow rates, variation in atomizer air pressure (over the range 10 to 30 psig) significantly changed combustion and emission characteristics.

The value of s along the burner length was determined from measured O_2 concentrations when the mean equivalence ratio was stoichiometric. Under these conditions, once combustion of the hydrocarbon fuels has occurred, any significant average O_2 concentration in the burnt gases is the result of imperfect mixing. Increasing the atomizer air pressure reduced s, flame luminosity and CO emissions at a given $\bar{\phi}$. The effect on NO emissions depended on the value of $\bar{\phi}$. These s profiles were used to calculate NO and CO concentrations along the burner length; these agreed well with measured values. Turbulent mixing theory was used to relate the decay of s with time (or distance along the burner) to a mixing rate intensity I as

$$s^2(t) = s_o^2 \exp(-It) \qquad (12)$$

It was found that I varied approximately as the square of the atomizing air pressure[28]. A simple model which assumed that the mixing rate intensity I was proportional to the one third power of the kinetic energy of the air entering the burner reaction zone predicted a one third power dependence of I on atomizing air pressure. This disagreement suggests that effects of atomizer air pressure on fuel droplet size, droplet velocity, and spray cone angle are likely to be important. This is obviously an area for

further work; the success of the mixing model in a simpler flow geometry is, however, encouraging.

A number of experimental studies in gas turbine combustors have shown that changing fuel injection techniques in a manner expected to reduce nonuniformities in the primary zone has reduced soot, CO, hydrocarbon and NO emissions. Norster and Lefebvre[29] have compared a dual-orifice atomizer and an "air spray" atomizer. Grobman[4] has presented results showing how increasing the pressure drop across an air-assist fuel nozzle can significantly reduce CO and HC emissions and improve combustion efficiency. Dix and Bastress[30] have shown that increasing the air pressure drop across the air-assist fuel nozzle in an automotive gas turbine with a fuel-lean primary zone significantly decreases NO emissions. This corresponds to reducing s_o in the NO prediction model, and Figure 4 indicates that for a lean system a substantial decrease in the NO formation rate would be expected.

Several combustor performance parameters in addition to emissions--combustion efficiency, blow-out, relight characteristics, primary zone soot formation and wall radiative heat flux--are also influenced by the extent of the fuel-air nonuniformities in the primary and secondary zones. Dix and Bastress[30] have already suggested how some of these performance parameters might be related to the mixing parameter s. It is therefore desirable that the role of nonuniformities in gas turbine combustors receive the utmost attention, both theoretically and experimentally.

4. NO_x EMISSIONS FROM THE NASA SWIRL CAN COMBUSTOR

To illustrate the versatility of the NO prediction model, we have applied it to a new combustor concept which shows promise of lower emissions. This concept, the NASA modular swirl can combustor Model 4-C, is an unconventional annular design.[4][11] Fuel is introduced into 120 swirl cans mounted in three concentric rings at the same axial station. Most of the air flows through these modules and in between them at the plane of the "blockage plates" which are the maximum axial cross-sections of the swirl cans. Only about 6% of the total air flow (used as liner cooling air) does not pass through or between the swirl cans. Figure 10 shows the construction of a swirl can. Air flows from the left, entering the can and mixing with fuel, which is sprayed onto the swirler plate from a fuel tube inside the can. This fuel-air mixture passes through the swirler and burns in the wake of the module. Some of the air which has passed around the module is entrained into the recirculating wake flow. Cold-flow tests confirm that this recirculating wake extends approximately one blockage-plate diameter downstream. The air which flows around the module but is not entrained into this "primary zone" will mix with the combustion products from the primary zone further downstream. Figure 11 is a tangential view of the combustor showing the swirl can modules mounted at the entrance plane of the annular liner. At low fuel-air ratios the combustion occurs within small primary zones in the wake of each swirl can. As the fuel-air ratio approaches stoichiometric, the primary zones coalesce into a single "ring of fire."

The difficulty with analyzing the NASA combustor is that contrary to more conventional designs, the volume of the primary zone and the mass flow of air entering this zone are not well defined by the liner geometry. The fluid mechanics of entrainment into a reacting, swirling, recirculating flow are not tractable enough to be used in the relatively simple nitric oxide formation model being proposed here. The following simplifying assumptions are made to obtain a simple model applicable to combustion operation at low fuel-air ratios, i.e. not too close to the stoichiometric value of 0.067. (i) The volume of the primary zone in the wake of each swirl can module is taken to be 8.7 $in.^3$, which is equal to the area of an averaged blockage plate multiplied by the plate's diameter. This aspect ratio of approximately one is verified by cold-flow tests. If the flow patterns in the combustor do not change much as the volume flow rate and combustion intensity are varied, the volume of the primary zones will remain nearly constant. Of course, as the fuel-air ratio approaches stoichiometric and the primary zones coalesce, this assumption becomes invalid. (ii) The average fuel-air ratio in the primary zones is proportional to the combustor's overall fuel-air raiio. Once again, if the combustor's flow patterns remain relatively fixed, this assumption will be approximately true. (iii) The nitric oxide formation reactions are rapidly quenched as the combustion products leave the primary zones. Consider a burnt-gas eddy whose local fuel-air ratio is less than the fuel-air ratio with the peak nitric oxide formation rate. A relatively small amount of dilution (from the air flowing between the swirl cans which was not entrained into a primary zone) will cause the temperature-sensitive nitric oxide reactions to freeze. Therefore, this quenching assumption appears reasonable when most of the primary-zone burnt-gas eddies are leaner than approximately stoichiometric.

A few comments on the above modelling assumptions are in order. (i) Primary zone residence times vary inversely with primary zone volume. Nitric oxide production is found to be almost linear with residence time for the region of interest, so that changing the primary zone volume will approximate sliding the nitric oxide prediction curves vertically on a log scale. (ii) Changing the proportionality factor between the primary and overall fuel-air ratios is equivalent to changing the fraction of the overall air flow which enters the primary zone. This changes both the primary zone residence time and the dilution factor on exit from the primary zone. The approximate linearity of nitric oxide with residence time mentioned above results in a cancellation of the residence time and dilution factor effects. Thus, changing the proportionality factor between the primary and overall fuel-air ratios merely slides the nitric oxide predictions horizontally on a log scale of overall fuel-air ratio.

At overall fuel-air ratios comparable to stoichiometric, the flow model described above clearly must be changed. (Even if the concept of 120 module-wake primary zones remained valid, these primary zones would be operating at fuel-air ratios well above stoichiometric and produce negligible nitric oxide compared to what would be formed during dilution to the overall fuel-air ratio.) A better model is to treat the entire combustor annulus inside the liner as a partially stirred reactor, driven by the swirlers and blockage plates at the entrance plane and the high combustion intensity. The model corresponds to the "ring of fire" flow pattern observed at high fuel-air ratio operating conditions. The swirl-cans then serve as crude versions of an air-assisted fuel injector, partially premixing the fuel before combustion with the main air flow. The combustion zone volume of interest for the high fuel-air operating conditions is approximately 4.1 $ft.^3$, the entire annulus within the combustor liner. The average fuel-air ratio is about 1.03 times the overall value, to allow for adding half of the 6% of total air flow used to cool the

liner. The sampled exhaust gases were quenched at the combustor exit by the sampling probe, so downstream quenching is not considered in the calculations.

Figures 12, 13 and 14 are comparisons of measurements on the swirl can combustor reported by Niedzwiecki and Jones[11] with computations made using the two models described in this section. The data points shown as circles are measurements made at a combustor inlet pressure of 5 to 6 atma, with a combustor air flow of 85 to 110 lbm/sec. The data points shown as diamonds are known to be measured at 6 atma and 110 lbm/sec., which were the values used in the analytical computation.

The curves drawn for fuel-air ratios between 0.01 and 0.03 are calculated with the low fuel-air ratio model (120 separate primary zones), using a primary zone fuel-air ratio of 2.5 times the overall value. As mentioned earlier, a change in this parameter will simply proportion out the prediction curves horizontally. Also note that a change in primary zone volume simply shifts the curves vertically. The mixing parameter values 0.33 and 0.42 which are illustrated produce approximately the proper slope to match the data, especially for the higher combustor inlet temperature cases, Figures 13 and 14.

The curves drawn for fuel-air ratios greater than 0.03 are calculated using the model appropriate to fuel-air ratios comparable with stoichiometric. Here the primary zone volume and fuel-air ratios are well defined, so that the prediction curves are not shiftable without making basic changes in the model.

Table 3 gives some of the parameters relevant to the nitric oxide calculations for a few sample points from the s = 0.33 curves presented in Figures 12, 13 and 14.

TABLE 3

Combustor Inlet Temperature, °F	Overall Fuel-Air Ratio	Primary Zone Fuel-Air Ratio	Primary Zone Residence Time, msec	Nitric Oxide from Primary Zone, mass-fraction
602	0.0160	0.0400	0.93	4.55×10^{-5}
907	0.0187	0.0467	0.83	2.10×10^{-4}
1058	0.0214	0.0534	0.76	3.97×10^{-4}
602	0.0650	0.0669	1.89	2.20×10^{-4}
907	0.0500	0.0515	2.02	5.61×10^{-4}
1058	0.0400	0.0412	2.16	4.72×10^{-4}

The two models described in this section match the lean and rich ends of the NASA emissions data reasonably well. To cover the middle range of fuel-air ratios would require modelling the air entrainment and mixing processes. This goes beyond our present understanding of the processes occurring within the combustor. However, curves which are simply faired in between the model prediction curves of Figures 12, 13 and 14 produce good matches with the experimental data.

To show the use of the nitric oxide formation model in extrapolating experimental data, calculations were made for operation of the NASA combustor at sea level static dry takeoff conditions typical of combustors used in state-of-the art engines in the 40,000-pound + thrust class. Table 4 gives results based upon the following data: combustion inlet temperature = 1400 °R, combustor pressure = 23 atma, overall fuel-air ratio = 0.023, primary zone fuel-air ratio = 0.0575, mixing parameter s = 0.33. A correction factor of 1.25 is used to approximately compensate for the divergence of the s = 0.33 curve from the data at a fuel-air ratio of 0.023 as the rapid quench assumption becomes inadequate.

TABLE 4

Reference Velocity ft./sec.	Nitric Oxide, mass fraction at exhaust	Emissions Index lbm NO_2/1000 lbm fuel	"Corrected" Emissions Index
75	3.15×10^{-4}	21.5	26.9
100	2.56×10^{-4}	17.4	21.8
125	2.16×10^{-4}	14.7	18.4

5. CONCLUSIONS

(i) The nitric oxide formation process in conventional gas turbine combustors is now reasonably understood. The parameters important in determining exhaust NO concentrations are inlet air pressure and temperature, mean primary zone residence time and fuel air ratio, the uniformity of the fuel-air ratio distribution in the high temperature zones in the combustor and the air dilution rate at the upstream end of the secondary zone.

(ii) The model for predicting NO emissions we have described can match measured emissions data from several different types of combustor over a wide range of operating conditions. The major problem in applying the model is that the parameter characterizing the fuel-air ratio nonuniformities must be determined empirically. The potential for relating this parameter to injection and combustor design and operating parameters has already been demonstrated in simpler flow geometries. This is an area for intensive analytical and experimental research.

(iii) The NASA swirl can combustor concept, through a reduction of high temperature zone residence time, and leaner and better mixed primary zone compared with current conventional combustors, has achieved a significant reduction in NO emissions when compared with current "jumbo jet" engines.

6. REFERENCES

1. Anon. Aircraft Emissions: Impact on Air Quality and Feasibility of Control, U.S. Environmental Protection Agency, Dec. 1972.

2. Federal Register, vol. 37, No. 239, Part II, Dec. 12, 1972, p. 26491.

3. Barrington, A. E., ed., Climatic Impact Assessment Program: Proceedings of the Survey Conference, Feb. 15-16, 1972, Cambridge, Mass., U.S. Dept. of Transportation, 1972.

4. Grobman, J. S., "Effect of Operating Variables on Pollutant Emissions from Aircraft Turbine Engine Combustors," Emissions from Continuous Combustion Systems, ed. by Cornelius, W., and Agnew, W. G., Symposium held at General Motors Research Laboratory, Warren, Michigan, Sept. 27-28, 1971, Plenum Press, 1972, pp. 279-303.

5. Bahr, D. W., "Technology for the Reduction of Aircraft Turbine Engine Exhaust Emissions," AIAA Paper No. 72-1202, AIAA/SAE 8th Propulsion Joint Specialists Conference, New Orleans, Nov. 29-Dec. 1, 1972.

6. Fletcher, R. S., and Heywood, J. B., "A Model for Nitric Oxide Emissions from Aircraft Gas Turbine Engines," AIAA Paper No. 71-123, presented at AIAA 9th Aerospace Sciences Meeting, N.Y., Jan. 25-27, 1971.

7. Mikus, T., and Heywood, J. B., Comb. Sci. Tech., vol. 4, 1971, pp. 149-158.

8. Fletcher, R. S., Siegel, R. D., and Bastress, E. K., The Control of Oxides of Nitrogen Emissions from Aircraft Gas Turbine Engines, vol. I, Report No. 1162-1, Northern Research and Engineering Corporation, Cambridge, Mass., Dec. 1971.

9. Hammond, D. C., and Mellor, A. M., Comb. Sci. Tech., vol. 4, 1971, pp. 101-112.

10. Roberts, R., Aceto, L. D., Kollrack, R., Bonnell, J. M., and Teixeira, D. P., "An Analytical Model for Nitric Oxide Formation in a Gas Turbine Combustion Chamber," AIAA Paper No. 71-715, AIAA/SAE 7th Propulsion Joint Specialist Conference, Salt Lake City, June 14-18, 1971.

11. Niedzwiecki, R. W., and Jones, R. E., "Pollution Measurements of a Swirl Can Combustor," AIAA Paper No. 72-1201, AIAA/SAE 8th Joint Propulsion Specialist Conference, New Orleans, Nov. 29-Dec. 1, 1972.

12. Heywood, J. B., Fay, J. A., and Linden, L. H., AIAA J., vol. 9, No. 5, 1971, pp. 841-850.

13. Heywood, J. B., "Gas Turbine Combustor Modelling for Calculating Nitric Oxide Emissions," AIAA Paper No. 71-712, AIAA/SAE 7th Propulsion Joint Specialist Conference, Salt Lake City, June 14-18, 1971.

14. Westenberg, A. A., Comb. Sci. Tech., vol. 4, Issue 2, 1971, pp. 59-64.

15. Morr, A., "A Model for Carbon Monoxide Emissions from Industrial Gas Turbine Engines," Ph.D. Thesis, M.I.T., Feb. 1973.

16. Baulch, D. L., Drysdale, D. D., Home, D. G., and Lloyd, A. C., Critical Evaluation of Rate Data for Homogeneous Gas Phase Reactions of Interest in High Temperature Systems, Part 4, Dept. of Chem., The University, Leeds, Dec. 1969.

17. Campbell, I. M., and Thrush, B. A., Trans. Faraday Soc., vol. 64, 1968, pp. 1265-1274.

18. Mellor, A. M., "Current Kinetic Modelling Techniques for Continuous Flow Combustors," Emissions from Continuous Combustion Systems, ed. Cornelius, W., and Agnew, W. A., Symposium held at General Motors Research Laboratory, Warren, Michigan, Sept. 27-28, 1971, Plenum Press, 1972, pp. 23-49.

19. Appleton, J. P., and Heywood, J. B., "The Effect of Imperfect Fuel-Air Mixing in a Burner on NO Formation from Nitrogen in the Air and the Fuel," 14th Symposium (International) on Combustion, Penn State, August 1972, to be published by the Combustion Institute.

20. Edelman, R., and Economos, C., "A Mathematical Model for Jet Engine Combustor Pollutant Emissions," AIAA Paper No. 71-714, AIAA/SAE 7th Propulsion Joint Specialist Conference, Salt Lake City, June 14-18, 1971.

21. Pratt, D. T., Bowman, B. R., Crowe, C. T., and Sonnichsen, T. C., "Prediction of Nitric Oxide Formation in Turbojet Engines by PSR Analysis," AIAA Paper No. 71-713, AIAA/SAE 7th Propulsion Joint Specialist Conference, Salt Lake City, June 14-18, 1971.

22. Jackson, S. R., and Odgers, J., "Factors Influencing Heat Release in Combustion Chambers and Consideration of the Related Materials and Structures," Combustion in Advanced Gas Turbine Systems, ed. Smith, I. E., London, Pergamon Press, 1968, pp. 137-208.

23. Grobman, J. S., Comparison of Calculated and Experimental Total-Pressure Loss and Airflow Distribution in Tubular Turbojet Combustors with Tapered Liners, NACA Memo 11-26-58E, National Advisory Committee for Aeronautics, 1958.

24. Norster, E. R., and Lefebvre, A. H., "Influence of Fuel Preparation and Operating Conditions on Flame Radiation in a Gas Turbine Combustor," ASME Paper No. 72-WA/HT-26, ASME Winter Annual Meeting, New York, Nov. 26-30, 1972.

25. Cornelius, W., Stivender, D. L., and Sullivan, R. E., "A Combustion System for a Vehicular Regenerative Gas Turbine Featuring Low Air Pollutant Emissions," SAE Paper 670936, SAE Combined Fuels and Lubricants, Power Plant and Transportation Meeting, Pittsburgh, 1967.

26. Cornelius, W., and Wade, W. R., "The Formation and Control of Nitric Oxide in a Regenerative Gas Turbine Burner," SAE Paper 700708, SAE Combined Farm, Construction and Industrial Machinery and Power Plant Meetings, Milwaukee, Wisconsin, 1970.

27. Pompei, F., and Heywood, J. B., Comb. Flame, vol. 19, to be published 1972.

28. Flagan, R., M.I.T. Ph.D. Thesis, to be submitted June 1973.

29. Norster, E. R., and Lefebvre, A. H., "Effects of Fuel Injection Method on Gas Turbine Combustor Emissions," Emissions from Continuous Combustion Systems, ed. Cornelius, W., and Agnew, W. A., Symposium held at General Motors Research Laboratory, Warren, Michigan, Sept. 27-28, 1971, Plenum Press, 1972, pp. 255-278.

30. Dix, D. M., and Bastress, E. K., "Approaches to Design of Low-Emission Gas-Turbine Combustion Chambers," SAE Paper 720728, SAE National Combined Farm, Construction and Industrial Machinery and Power Plant Meetings, Milwaukee, Wisconsin, Sept. 11-14, 1972.

ACKNOWLEDGMENT

This work was supported in part by the National Aeronautics and Spece Administration under Grant NGL 22-009-378.

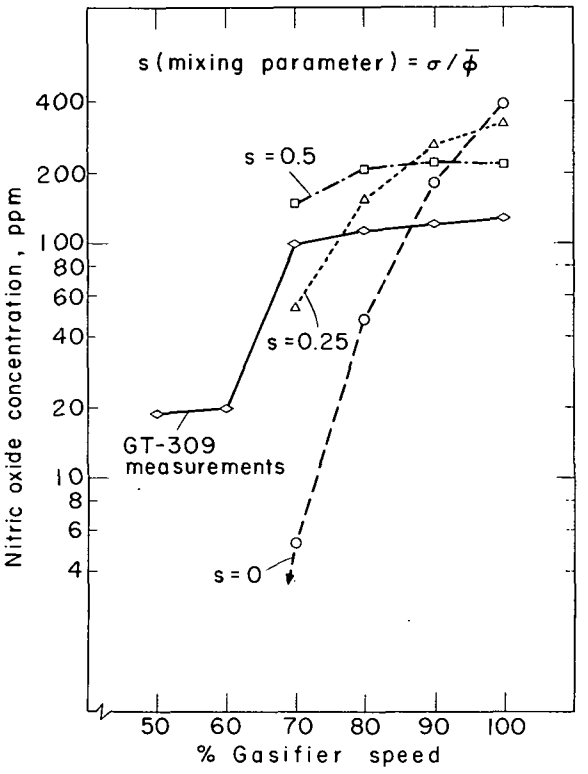

Fig. 8. Theoretical calculations of General Motors GT-309 engine combustor NO emissions versus gasifier speed, compared with engine exhaust measurements(7).

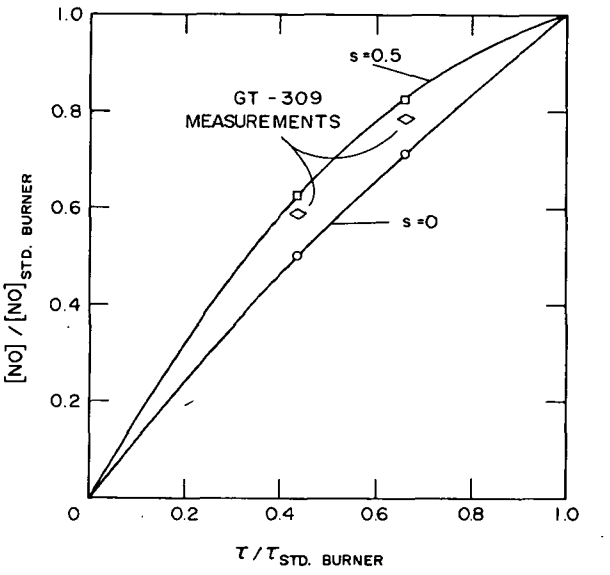

Fig. 9. Theoretical calculations of GT-309 combustor design-point NO emissions versus mean primary zone residence time, compared with measured values for the standard (std.) burner and two early quench design modifications(7).

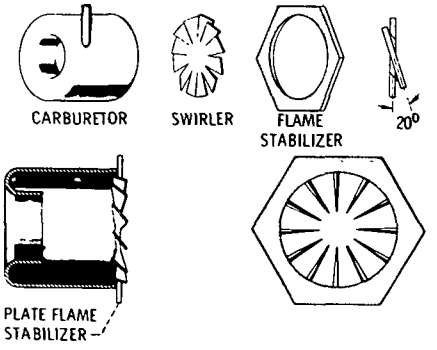

Fig. 10. NASA swirl can combustor module details(4).

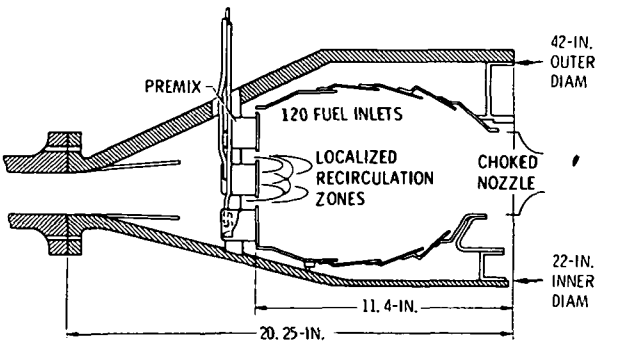

Fig. 11. NASA modular swirl can combustor schematic layout(4).

Fig. 12. Comparison of measured and predicted NO mass fractions at exit of NASA swirl can combustor as a function of overall fuel-air ratio. Curves at lower left are from single module model appropriate for low fuel-air ratios. Curves at upper right are from high fuel-air ratio model treating entire combustor as the primary zone. Data points shown as circles are measurements made at pressures of 5 to 6 atm with a combustor airflow of 85 to 110 lbm/sec. Data points shown as diamonds are at 6 atm and 110 lbm/sec, the values used in the computations. Nominal combustor inlet temperature is 600 °F. Data from Niedzwiecki and Jones[11].

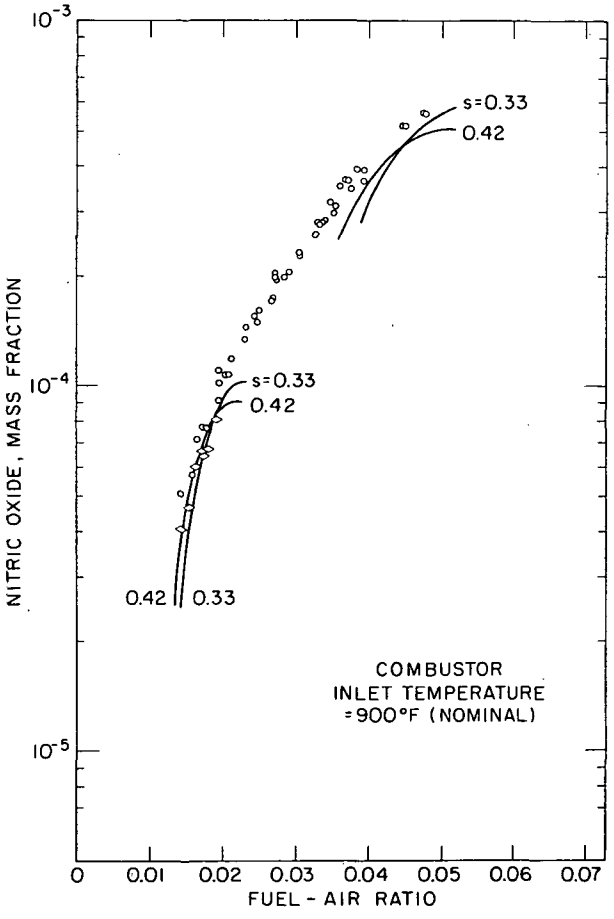

Fig. 13. Same as Figure 12 with nominal combustor inlet temperature of 900 °F.

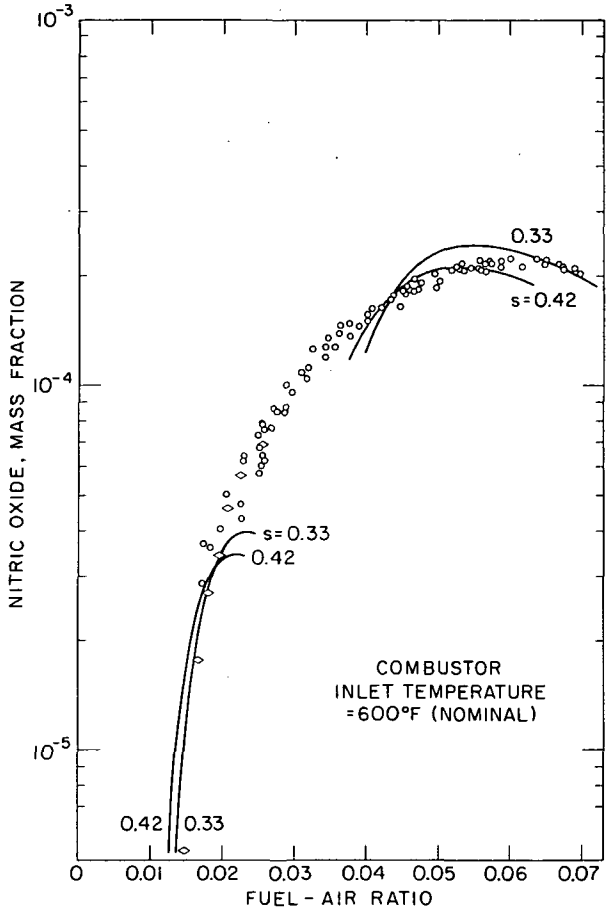

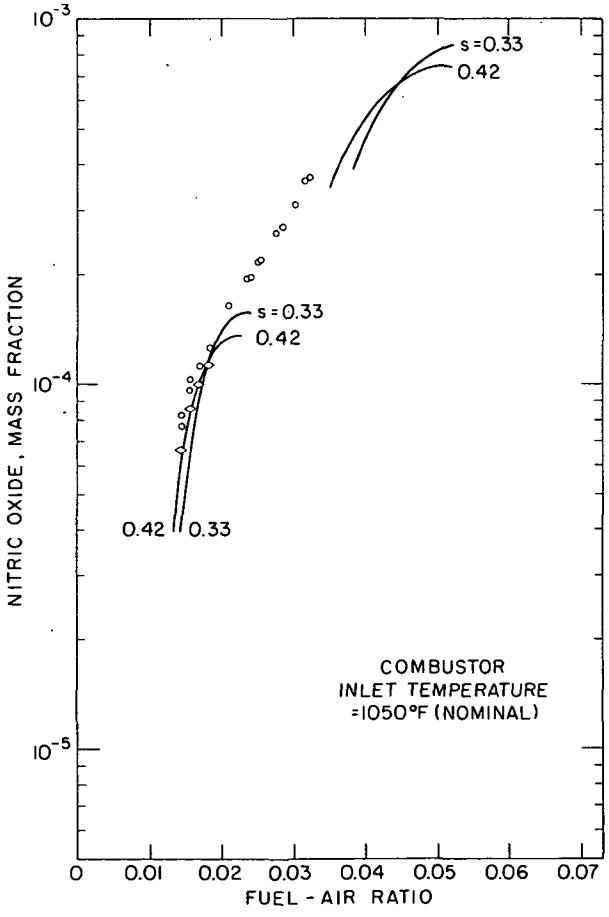

Fig. 14. Same as Figure 12 with nominal combustor inlet temperature of 1050 °F.